

Reaction dynamics of proton drip-line nuclei at energies around the Coulomb barrier

C. Chang¹, L. Yang^{1*}, C. J. Lin^{1**}, H. Yamaguchi², N. R. Ma¹, S. Hayakawa², P. W. Wen¹, H. M. Jia¹, T. P. Luo¹, C. Yin¹, Z. J. Huang¹, H. R. Duan¹, S. X. Zhu¹, H. R. Wang¹, Z. R. Fan¹, H. Y. Li¹, and L. Y. Fu¹

¹China Institute of Atomic Energy, PO Box 275 (10), Beijing 102413, China

²Center for Nuclear Study, University of Tokyo, RIKEN campus, 2-1 Hirosawa, Wako, Saitama 351-0198, Japan

Abstract. This work briefly introduces our recent studies on reactions induced by proton drip-line nuclei, ^8B and ^{17}F , at energies around the Coulomb barrier. Using detector arrays with large solid-angle coverage, the complete kinematics measurements were performed for systems of $^8\text{B}+^{120}\text{Sn}$ and $^{17}\text{F}+^{58}\text{Ni}$. For the $^8\text{B}+^{120}\text{Sn}$, the coincident measurement of the breakup fragments was achieved for the first time for a proton-halo nuclear system. The correlations between the breakup fragments reveal that the prompt breakup occurring on the outgoing trajectory dominates the breakup dynamics of ^8B . For $^{17}\text{F}+^{58}\text{Ni}$, the complete reaction channel information, such as quasi-elastic scattering, breakup and total fusion, was derived for the first time. An enhancement of the fusion cross section of $^{17}\text{F}+^{58}\text{Ni}$ was observed at the energy below the Coulomb barrier. Theoretical calculations indicate that this phenomenon is mainly due to the couplings to the continuum states. Moreover, different direct reaction dynamics were found in ^8B and ^{17}F systems, suggesting the influence of proton-halo structure on the reaction dynamics.

1 Introduction

Nuclei located closed to the drip line may present exotic phenomenon, such as the “halo” structure, which was first discovered by Tanihata *et al.* [1] in nucleus ^{11}Li . The extremely extended matter distributions result in a weakly-bound structure, a manifestation of which is the large breakup probability in nuclear collisions. It becomes more intriguing when the interaction energy gets close to the Coulomb barrier region, where couplings to the breakup continuum states turn to be significant [2]. Therefore, the influence of the weakly-bound structure on the reaction dynamics at energies close to the Coulomb barrier has become one of the most popular topics in the field of nuclear physics [2, 3].

The reaction dynamics induced by neutron-halo nuclei has been investigated extensively both experimentally and theoretically at near-barrier energies [3]. Compared to their neutron counterparts, a proton halo system may exhibit distinctive reaction properties, since the valence proton actively participates in the reaction due to the Coulomb interaction between the proton and the core as well as the proton and the target. Owing to the limitation of the secondary beam quality, however, corresponding experimental data on proton-halo systems are rather scarce. Therefore, the reaction mechanisms of proton halo nuclear systems are still elusive to date. To further investigate the reactions induced by proton drip-line nuclei, we performed the first complete kinematics measurement

of $^8\text{B}+^{120}\text{Sn}$ [4] and $^{17}\text{F}+^{58}\text{Ni}$ [5] at energies around the Coulomb barrier. The proton separation energy of ^8B is merely 138 keV, exhibiting an exotic proton-halo structure. More intriguing, ^8B is one of the few cases that whose ground state present a proton halo [6]. For ^{17}F , it has a breakup threshold of 600 keV into $^{16}\text{O}+\text{p}$. The first excited state ($E_x=495$ keV, $J^\pi=1/2^+$) of ^{17}F has been reported to present a proton halo structure, which is bound by only 105 keV. The description of the experiments and discussions will be given in the following sections.

2 The $^8\text{B}+^{120}\text{Sn}$ measurement

The experiment was performed at two energies of 37.8 ± 0.5 and 46.1 ± 0.6 MeV [4] at CRIB (CNS Radioactive Ion Beam separator) [7] of the Center for Nuclear Study (CNS), the University of Tokyo. Using a silicon detector array with a large solid-angle coverage, the correlations between the breakup fragments ^7Be and proton were derived for the first time at low interaction energies, which is essential to pin down the breakup dynamics of a proton-halo system. The angular distributions of exclusive and inclusive breakup of $^8\text{B}+^{120}\text{Sn}$ are found to be nearly identical with each other within the uncertainties, indicating that the elastic breakup (EBU) is the dominant direct reaction process. The contribution of non-elastic breakup (NEB) was estimated by the IAV model [8] calculations, and the results indicate that NEB just contributes $\sim 18\%$ of the total ^7Be yield.

The reconstructed relative energy (E_{rel}) distribution of $^7\text{Be}+\text{p}$ at 38.7 MeV is shown in Fig. 1 (a), where the cir-

*e-mail: yang_lei@cinae.ac.cn

**e-mail: cjlin@cinae.ac.cn

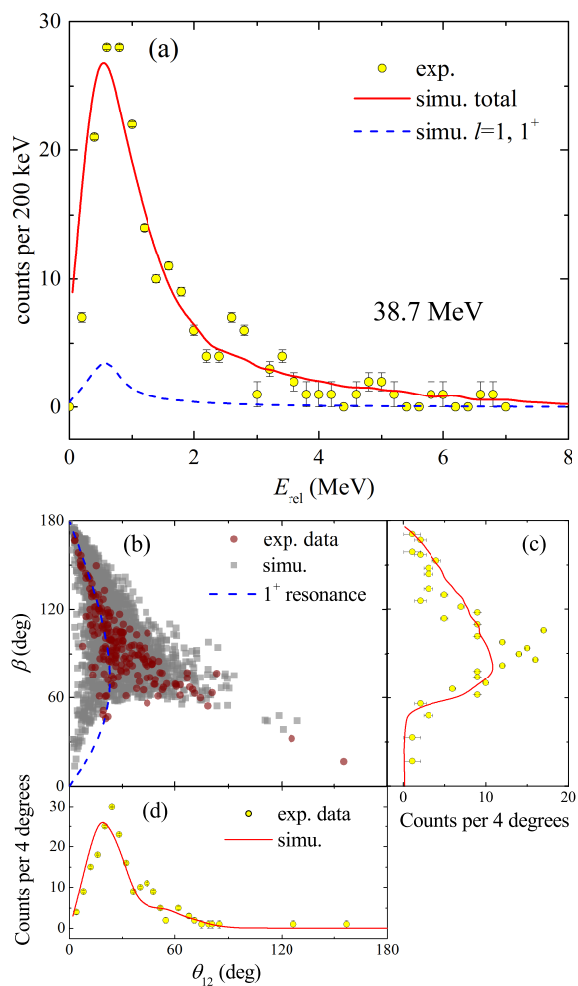


Figure 1. (a) The measured E_{rel} distribution for breakup fragments ${}^7\text{Be}$ and proton at 38.7 MeV and compared with the simulation results (solid curves). The dashed curves denote simulation results of p -wave 1^+ state. (b) Comparison of experimental data (circles) with simulations (squares) for β vs θ_{12} at 38.7 MeV. The dashed curve shows the expected β - θ_{12} correlation assuming asymptotic breakup from the 1^+ resonance of ${}^8\text{B}$. The projections of β and θ_{12} are shown in panels (c) and (d), respectively. The solid curves denote the simulations results. The figures are taken and modified from Ref. [4].

cles an solid curve denote the experimental results and the simulations based on the continuum-discretized coupled-channels (CDCC) [9] calculations, respectively. One can see that the simulation result reproduce the data successfully. A distinctive peak is observed at around 600 keV in the E_{rel} distribution, which is very close to the location of the first resonant state of ${}^8\text{B}$ ($E_x=770$ keV, $J^\pi=4^+$, $\Gamma=35.6$ keV). CDCC calculation was performed to estimate the contribution of this $l=1$ resonance. The result suggests that this resonance only contribute $4.4\pm 2.0\%$ at 38.7 MeV. The simulation result for the $l=1$ resonance is shown in Fig. 1 by the dashed line as well. The small fraction of the first resonant state contribution suggests that the prompt breakup is the dominant breakup mechanism for ${}^8\text{B}$. The angular correlation, i.e., θ_{12} - β , as well as the distributions of β and θ_{12} at 38.7 MeV are shown, respectively, in Fig. 1

(b), (c) and (d). θ_{12} denotes the opening angle between the breakup fragments, and β represents the orientation of the relative momentum of breakup fragments in their center-of-mass frame [10]. Circles are the experimental data, and squares and solid curves denote the simulations based on the CDCC calculations. It can be found that the simulations reproduce the date reasonably well. Moreover, the expected correlation between θ_{12} and β assuming the breakup via the 1^+ long-lived resonance of ${}^8\text{B}$ is shown by the dashed curve in Fig. 1 (b). One can see that a majority of the events deviate from the dashed curve, confirming that breakup through the the first resonance is just a minor contributor. Furthermore, a strongly forward-peaked structure is observed in the θ_{12} distribution, suggesting that breakup mainly occurs in the outgoing trajectory of ${}^8\text{B}$, in which case, the initial velocities of the fragments are in the same direction as the Coulomb interaction from the target nucleus, leading to a small θ_{12} . Similar results were obtained as well for the higher energy case, 46.1 MeV. More details can be found in Ref. [4].

3 The ${}^{17}\text{F}+{}^{58}\text{Ni}$ measurement

The experiment of ${}^{17}\text{F}+{}^{58}\text{Ni}$ was performed at CRIB as well at four near-barrier energies, 43.06 ± 0.7 , 47.5 ± 0.7 , 55.7 ± 0.8 and 63.1 ± 0.9 MeV [5]. A Multi-layer Ionization-chamber Telescope Array (MITA) [11] was developed to identify the relatively heavy breakup fragment ${}^{16}\text{O}$ with low energies. Thanks to the powerful capability of particle identification of MITA, the information of various reaction channels, such as quasi-elastic scattering, inclusive and exclusive breakup, as well as the total fusion reaction were derived. For the breakup angular distributions, CDCC and IAV model calculations were performed to interpret the data. The results show that CDCC can reasonably reproduce the exclusive ${}^{16}\text{O}$ angular distributions, and the sum of CDCC and IAV, which can be referred to as the total breakup, describes properly the inclusive data. Moreover, the IAV model calculations indicate that the NEB component is dominant in the ${}^{16}\text{O}$ production. Furthermore, the excitation function of total fusion reaction is shown in Fig. 2 (a), and compared with the results of ${}^{16}\text{O}+{}^{58}\text{Ni}$ [12]. One can see that, an enhancement is observed in the total fusion cross section of ${}^{17}\text{F}+{}^{58}\text{Ni}$ at the energy below the Coulomb barrier. CDCC results with and without the couplings to continuum states are shown in Fig. 2 (b) respectively by the solid and dashed curves. Details of the calculations can be found in Ref. [5]. One can see that the enhancement of the total fusion cross section below the Coulomb barrier mainly arises from the couplings to the breakup continuum states.

4 Discussion

Distinct reaction dynamics were found for ${}^8\text{B}$ and ${}^{17}\text{F}$ nuclear systems: for ${}^8\text{B}$, the exclusive breakup data clearly indicate that the EBU dominates the direct reaction mechanism, while NEB becomes the major component for ${}^{17}\text{F}+{}^{58}\text{Ni}$. To shed more light on this phenomenon, the ratio of exclusive breakup cross section to the total reaction

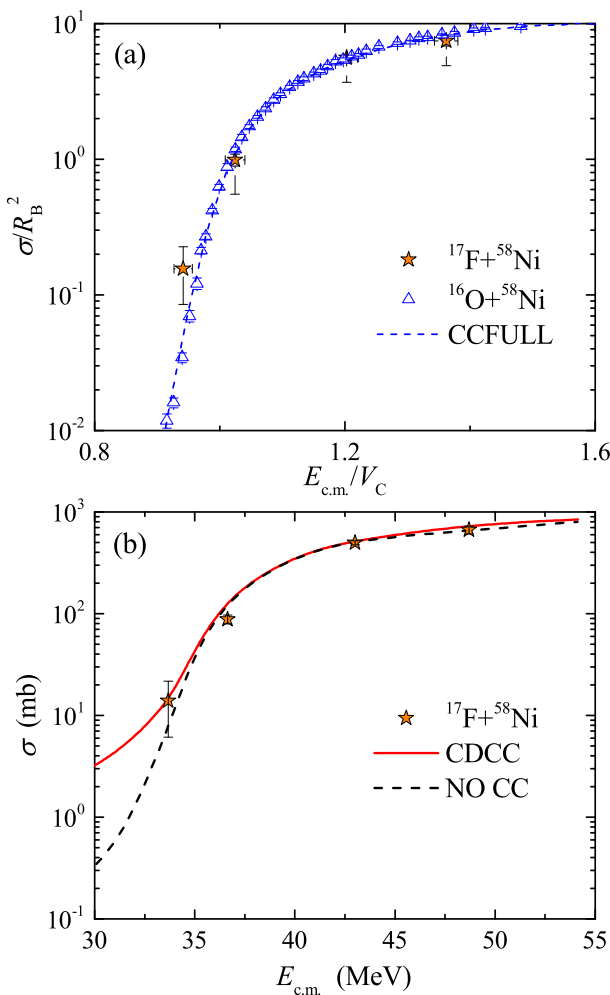


Figure 2. Comparison of the reduced total fusion excitation function of $^{17}\text{F}+^{58}\text{Ni}$ (stars) and $^{16}\text{O}+^{58}\text{Ni}$ (triangles) is shown in (a). The dashed curve denotes the CCFULL calculation for $^{16}\text{O}+^{58}\text{Ni}$. Calculations with and without (No CC) couplings to continuum states are shown in (b) respectively by solid and dashed curves, and compared with the fusion data of $^{17}\text{F}+^{58}\text{Ni}$ denoted by stars.

cross section vs. the breakup threshold of indicated systems are presented in Fig. 3, where the results of proton- and neutron-halo systems are respectively presented by solid and empty symbols. The data of ^8B and ^{17}F are taken from the present work, and those for neutron-halo systems are taken from references.

As shown in Fig. 3, the breakup probability decreases as the breakup threshold increases. Moreover, for a given breakup threshold, the proton-halo system show a smaller breakup probability than that of the neutron-halo system. That is mainly due to the additional Coulomb barrier, which does not exist for neutron. Further investigation is deserved from the experimental and theoretical point of view to understand the difference between the proton- and neutron-halo reaction systems systematically and comprehensively.

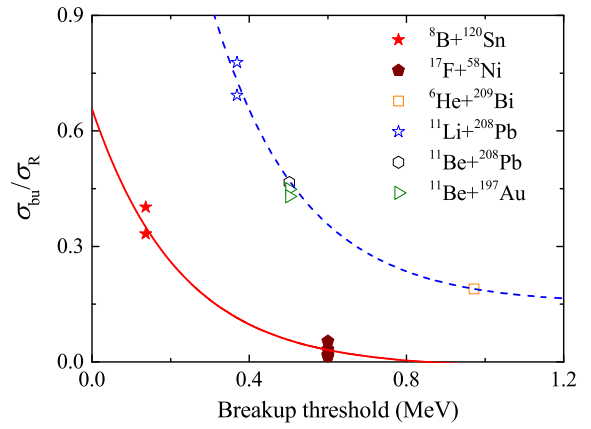


Figure 3. Ratio of breakup cross section to the total reaction cross section vs. the breakup threshold of indicated systems. The empty and solid symbols denote the results of neutron- and proton-halo systems, respectively. The lines are used to guide the eyes.

References

- [1] I. Tanihata, H. Hamagaki, O. Hashimoto, Y. Shida, N. Yoshikawa, K. Sugimoto, O. Yamakawa, T. Kobayashi, N. Takahashi, Phys. Rev. Lett. **55**, 2676 (1985)
- [2] L.F. Canto, P.R.S. Gomes, R. Donangelo, J. Lubian, M.S. Hussein, Phys. Rep. **596**, 1 (2015)
- [3] J.J. Kolata, V. Guimaraes, E.F. Aguilera, Eur. Phys. J. A **52**, 123 (2016)
- [4] L. Yang, C.J. Lin, H. Yamaguchi, A.M. Moro, N.R. Ma, D.X. Wang, K.J. Cook, M. Mazzocco, P.W. Wen, S. Hayakawa et al., Nat. Commun. **13**, 7193 (2022)
- [5] L. Yang, C.J. Lin, H. Yamaguchi, J. Lei, P.W. Wen, M. Mazzocco, N.R. Ma, L.J. Sun, D.X. Wang, G.X. Zhang et al., Physics Letters B **813**, 136045 (2021)
- [6] G.A. Korolev, A.V. Dobrovolsky, A.G. Inglessi, G.D. Alkhazov, P. Egelhof, A. Estradé, I. Dillmann, F. Farinon, H. Geissel, S. Ilieva et al., Phys. Lett. B **780**, 200 (2018)
- [7] Y. Yanagisawa, S. Kubono, T. Teranishi, K. Ue, S. Michimasa, M. Notani, J.J. He, Y. Ohshiro, S. Shimoura, S. Watanabe et al., Nucl. Instrum. Methods Phys. Res. A **539**, 74 (2005)
- [8] M. Ichimura, N. Austern, C.M. Vincent, Phys. Rev. C **32**, 431 (1985)
- [9] N. Austern, Y. Iseri, M. Kamimura, M. Kawai, G. Rawitscher, M. Yahiro, Phys. Rep. **154**, 125 (1987)
- [10] E.C. Simpson, K.J. Cook, D.H. Luong, S. Kalkal, I.P. Carter, M. Dasgupta, D.J. Hinde, E. Williams, Phys. Rev. C **93**, 024605 (2016)
- [11] N.R. Ma, L. Yang, C.J. Lin, H. Yamaguchi, D.X. Wang, L.J. Sun, M. Mazzocco, H.M. Jia, S. Hayakawa, D. Kahl et al., Eur. Phys. J. A **55**, 87

(2019)

[12] N. Keeley, J.S. Lilley, J.X. Wei, M. Dasgupt, D.J. Hinde, J.R. Leigh, J.C. Mein, C.R. Morton, H. Tim-

mers, N. Rowley, Nucl. Phys. A **628**, 1 (1998)